JOURNAL OF MATERIALS SCIENCE 9 (1974) 1715–1736

Review
Radiation damage and electron microscopy of organic polymers

D. T. GRUBB
H. H. Wills Physics Laboratory, University of Bristol, Bristol, UK

A condensed description is given of the fundamental processes involved in radiation damage and the effects of radiation on the physical and chemical properties of organic materials, particularly polymers. It is shown that the radiation doses received by specimens in the electron microscope are extremely high, very much greater than those used in radiation chemistry experiments. Because of this, only qualitative predictions of behaviour in the electron microscope can be made. A number of authors have described the changes in the image or diffraction pattern of particular specimen types during observation in the electron microscope and their work is reviewed here. In general, contrast features in the image may disappear, due to loss of mass or crystallinity, or new features may appear due to distortion of ordered regions. The effects of radiation damage on attainable resolution, and possible methods of improving the resolution are then discussed.

1. Introduction

Specimens in the electron microscope are inevitably exposed to irradiation by electrons. A certain fraction of these electrons will interact with orbital electrons in the specimen and transfer energy to them. At normal accelerating voltages the excited states formed in metals and most other inorganic substances dissipate their energy as heat, and no permanent change occurs. In some inorganic salts and all organic substances, however, some fraction of the excited states decay to altered structures, giving permanent changes in the chemical and physical properties of the specimen. In general, some fraction of the mass is lost, the chemical composition changes and any long range order originally present is destroyed.

When organic material provides the image contrast, the appearance of the specimen changes considerably during observation in the electron microscope, because of radiation damage. The impermanence of the original appearance limits the possible resolution. After considerable irradiation – which may only take a short time in the microscope – the specimen stabilizes in a new form, resistant to further radiation. All of the initial structure of interest may have been destroyed by this time, but often it has not been destroyed, merely altered, and the image of the irradiated specimen can give much useful information if it can be properly interpreted.

Specimens which are stained or shadowed, so that the image contrast is produced not by the organic material but by heavy metal atoms, are much less sensitive to radiation effects. Thus biological specimens which are generally fixed and stained are less affected than polymers which are not. If a biological specimen is not stained, fixed or embedded it is very rapidly destroyed by the beam, and the structure collapses completely [2]. On the other hand, the structure in a rubber sample, stained and fixed with osmium tetroxide is well preserved [3].

2. Effects of irradiation on polymers

2.1. Fundamental processes

Radiation affects materials by the deposition of energy. It is deposited discontinuously, in discrete amounts, and the average transfer at each interaction is large compared to the energy of chemical bonds. Gamma rays, electrons and heavier charged particles transfer the energy primarily by collision with electrons in the material, while for fast neutrons collisions with

atomic nuclei, particularly hydrogen, are most important. However, the displaced proton then loses its kinetic energy by interaction with many electrons in its path, so the difference in effect is not so very great. Fast electrons may interact initially with many electrons in the material, to give a collective excitation [4] but the lifetime of this excitation is very short, and it acts merely as a mcehanism for transferring energy within the material.

Once the energy is deposited at a single electron in the material, a large number of very rapid processes may occur. If the energy is sufficient, the electron is expelled from its orbit, leaving a positive ion. This ion is probably in an excited state and may be unstable, rapidly dissociating into free radicals or molecular fragments. If the expelled electron has little kinetic energy, it will be recaptured by its parent ion very quickly, in 10^{-11} sec or less, and the recapture produces a highly excited molecule. The excitation of energy 10 to 15 eV will cause the molecule to dissociate, and further chemical changes will result. Electrons expelled with more energy have several collisions near the primary event, producing a high concentration of reactive species in a small volume, called a spur. The electron loses its energy in this way, and in liquids it has a good chance of being recaptured by the ion. Only 10% of the ions produced are still in existence after 10^{-9} sec and 3% after 10^{-6} sec [5, 6]. In solids, the electrons are much more likely to be trapped. Positive ions diffusing by electron (or proton) transfer are likely to be localized near the trapped electrons, and will recombine at a rate controlled by the type of trap and the temperature of the system. If the electron has been captured to form a negative ion, the neutralization of ion pairs which occurs releases less energy than ion-electron recombination, so the end products are different. The radicals formed within the spur may recombine very quickly, in 10^{-8} sec or less, either to the original chemical structure, or to form a new one. Radicals which do not quickly recombine diffuse away in liquids, and combine with others much more slowly (in 10^{-3} sec, say). In a solid, diffusion is much slower and at low temperatures or in crystalline structures these radicals may be completely stable.

When the initial energy transfer is insufficient to form an ion pair, an excited state of the molecule will be induced. This may be an optically allowed state or a triplet, and it will have increased reactivity compared to the ground state. These excited states are much less energetic than those formed by charge neutralization, so dissociation is less likely. Light and heat will be produced as the excitations decay. The heat produced within a spur may be considerable, but it diffuses away very rapidly, at the speed of sound within the material [7] so that the temperature excess falls to a few percent of its initial value in 10^{-10} sec. "Initial" here means at some 10^{-12} sec after the first collision, when sufficient material reaches equilibrium for a temperature to be defined.

Study of the radiolysis of mixtures shows that energy absorbed by one molecule can be transferred to another by charge transfer, or as an excitation, even if the molecules are in limited contact [8]. Longer range energy transfer, up to 100 Å, can take place in the crystalline solid state [9]. Using compounds instead of mixtures shows that transfer from one part to another of the same molecule is more effective than that between molecules, so that one specific type of radical may form wherever the primary interaction with the molecule may be. A time scale of the fast processes so far described is given in Table I, adapted from Magee [10] and Williams [11].

The condensed and simplified account of the process of radiation damage given above shows that the situation is extremely complex, even when simple homogeneous systems are considered. For more detailed information see Ausloos [12], Spink and Woods [13] or Chapiro [14].

2.2. Chemical and physical effects

The exact nature of the product of irradiation will depend not only on the elemental composition of the starting material but on molecular configuration, conformation and size, and on the physical state, temperature, and impurity content of the system. At high doses, when a significant fraction of the material has been affected, the parameters of the material will have been changed, so more complications are introduced. None the less, there are several useful general results, which will now be described.

The process of energy transfer, and the very different sensitivities of different chemical structures result in specific bonds or types of bonds being disrupted when polyatomic molecules are irradiated. The bonds broken need not be those least stable energetically. The main site of bond

TABLE I

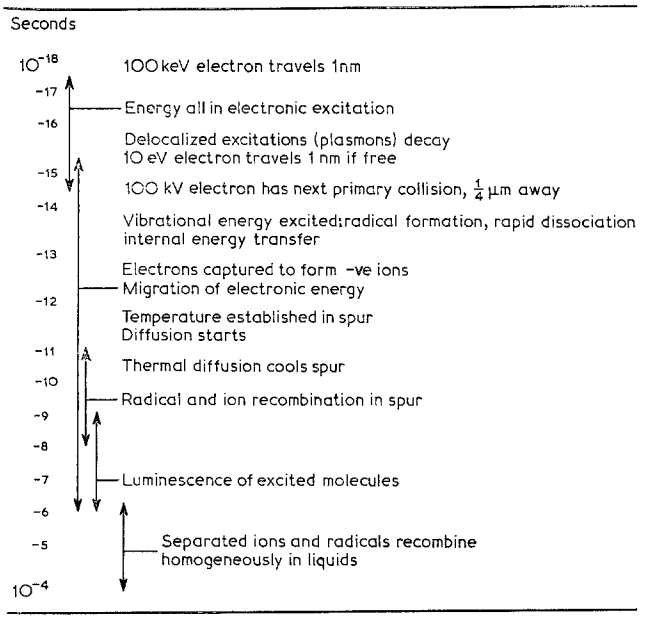

breakage for various types of compound is shown in Table II, adapted from Stenn and Bahr [15] and Hall *et al.* [16]. A very specific model for the case of polyethylene (PE) has been proposed by Partridge [17], where the excitation of a C–C bond is transferred rapidly along the chain, so that the energy is not localized at any one bond for a long enough time to break it. Excitation of C–H bonds is localized so that although they are stronger, they break.

If a bond which makes up part of the backbone of the molecule breaks, this main chain scission results in degradation, with products of a lower average molecular weight. If a carbon-hydrogen or carbon-halogen bond breaks then either another hydrogen is lost and unsaturation results, or the free valence joins with another on a different molecule. In polymers this process of two chains joining together is called cross-linking. Continued cross-linking causes the specimen to become a three dimensional network, which is an infusible and insoluble gel [18]. At very high doses the result is a hard and very brittle brown solid. Degradation causes the strength and melting point of the polymer to decrease, so that a liquid is eventually produced. Polymers can be divided into two main groups, those which cross-link and those which degrade. The first group include vinyl polymers of type a (Table II) polyesters, polamides and rubbers. The second includes vinyl polymers of type b (Table II) cellulose, polytetrafluoroethylene and polyethers [14]. Polymers are particularly sensitive to these changes because of their high initial molecular weight. A low molecular weight compound irradiated so that one molecule in 10 000 was cross-linked would be almost unaltered, with a tiny fraction of dimer. If the substance had been originally polymerized into long chains of 10 000 units each, then the same number of cross links, randomly placed, would cause a gel to form, altering the properties of the material drastically. The same argument applies for chain scission; instead of a negligible effect, the molecular weight would be halved.

A rapid formation of cross-links is often found at low doses which cannot be explained by the random formation of radicals in adjacent positions. The radicals must, therefore, migrate along the polymer chains and meet [19] most probably where they are trapped, or the excitations must migrate [17] and form radicals preferentially in certain regions. Some may be formed in pairs [20] but it cannot be simply that two radicals are formed in a spur and react quickly, because the radicals can be stabilized by cooling and removed chemically, and then no cross-links are formed on re-warming [21]. Comparative irradiation of bulk- and solution-crystallized PE [22, 23] showed that cross-links

TABLE II Chemical bonds most likely to be broken (bold lines) by irradiation in organic compounds

Compound	
Saturated hydrocarbons	—C—H or —C—C— depending on structure
in particular (a)	$\left[-CH_2-\underset{\displaystyle H}{\overset{\displaystyle R}{C}}- \right]_n$
(b)	$\left[-CH_2-\underset{\displaystyle R_2}{\overset{\displaystyle R_1}{C}}- \right]_n$
Unsaturated hydrocarbons	—C—H and C=C
Aromatic hydrocarbons	—C—H, —C—C— not in rings
Carboxylic acids	—C—H, —C—COOH
Ethers	—C—O—
Fluoride compounds	—C—H; —C—C— in $(CF_2)_n$, $(C_2F_3Cl)_n$
Other halogen compounds	When R is Cl in vinyl polymer type (a) above, —C—H and —C—C—. When R_1 and R_2 are Cl in type (b) —C—C—.
Amino acids	$H_2N-\underset{\displaystyle R}{\overset{\displaystyle H}{C}}-COOH$ which bond breaks depends on R

occur preferentially at the fold surfaces of lamellar crystals. The cross-links which are effective in reducing solubility are links between different lamellae and those not effective are links between different parts of the same molecule within one lamella, or links adjacent to those previously formed. Later work [24] using oxidative degradation and gel permeation chromatography to characterize irradiated material directly demonstrates that cross-links do not form in the crystal interior. An opposite result has been obtained, by comparison of

crystalline and amorphous PE at 133°C, which indicated that the crystalline material is more efficiently cross-linked by irradiation [25].

The simplest explanation for lack of cross-links within the crystal is the "cage effect". That is, the excited species produced are held more firmly in place when they are part of a crystalline lattice, so the probability of reformation of the original structure is greater and the amount of change produced is less. Irradiation at higher temperatures generally produces greater changes, probably for similar reasons. Reducing the temperature normally modifies and reduces but does not eliminate the effect of radiation [26, 27]. Whatever the state of the material, the probability of recombination to *almost* the original structure is quite high, and this leads to changes in conformation [28] and tacticity [29]. As radiation damage proceeds crystallinity is destroyed, and this can be observed directly by X-ray diffraction or by electron diffraction in the electron microscope, or indirectly by the depression of melting point [29]. On irradiation of PE, the density falls as crystallinity is reduced, but then rises as continued cross-linking leads to a tighter packing of the chains [30]. It was found that at 80°C about 400 Mrad of pile radiation destroyed crystallinity in PE [31] and about 3000 Mrad were required using 700 kV electrons [32] or gamma rays [33] at room temperature. A much lower dose inhibited the recrystallization of molten PE, even if the radiation was performed at room temperature and the polymer was then melted and cooled [34].

Aromatic compounds are much less sensitive to radiation than aliphatics, and in a compound a phenyl group can "protect" more sensitive groups over a distance of twelve carbon atoms [35]. Explanations for aromatic insensitivity have been given in terms of excitation levels [36] and in terms of delocalized resonances [37, 38]. The most resistant organic compounds so far discovered are the phthalocyanines and their derivatives. Copper phthalocyanine requires a hundred times greater dose than PE before the crystalline order is destroyed in the electron microscope and this substance gave the first resolution of lattice fringes, of 1nm spacing [39]. Chlorination of the sixteen peripheral CH groups increases the resistance by a further thirty times [40] and 0·5 nm resolution has been obtained on this compound [41].

Real polymer samples normally contain a wide range of molecular weight, and are often poorly characterized in terms of degree of branching, impurity content and state of order. It is not surprising that polymers of the same specification but from different sources should behave quite differently on irradiation nor that a lot of results await proper explanation. For further information on all the effects of radiation on polymers see the books by Charlesby [42] and Chapiro [14] and that edited by Dole [43]which contains much information which is more recent.

3. Radiation doses received in the electron microscope

The conventional unit of radiation dosage, the rad, is defined as 100 erg g^{-1} of absorbed energy. This unit was chosen because many chemical and biological effects of radiation on materials depend to a good approximation on the energy absorbed by unit mass, and not on the rate of absorption or on the type of ionizing radiation employed. The approximation is not so good in some cases because certain processes such as atomic displacement occur only when a threshold energy, much higher than the ionization energy, is exceeded [44, 45]. These processes are of low probability, and are important only when, as in metals, lower energy processes have no effect. Many processes are affected by the linear energy transfer rate (LET) along the path of the ionizing particle [33, 46] but not to any great extent. The absorbed energy would be very difficult to measure in the electron microscope, and normally the incident electron flux is measured instead, in units of coulombs per square metre or electrons per square nm.

Let the beam current collected by the final viewing screen by I, the area of the screen A, the magnification M and the time of exposure t. If these are determined under normal operating conditions but without the specimen in place (thus ensuring that all electrons in the beam at the specimen plane reach the screen) then the mean flux incident on the specimen equals $qItM^2/A$, where q is a correction factor for the collection efficiency of the screen [47, 48]. Alternatively, a permanent faraday cup can be fitted for which q is nearly 1 [49]. Using the flux arrived at in this way as a measure of dose would be misleading, for the absorbed energy depends on the beam voltage (being proportional to 1/(electron velocity)^2, which is approximately the same as

1/voltage, below 200 kV) and on the nature of the specimen.

The conversion factor between incident and absorbed energy for carbonaceous materials has been calculated by several authors, either from the Thomson-Whiddington law [50, 51] although it is not appropriate for a thin specimen, or directly from the Bethe law [52] which gives the energy loss rate of a 100 kV electron passing through carbonaceous material of density 1 g cm^{-3} as between 400 and 450 eV μm^{-1}, depending on the exact parameters chosen [53, 54, 15].

If 1 electron loses 400 eV μm^{-1}
then 1 C loses 400 J μm^{-1}
1 m^2 of the material, 1 μm thick, weighs 1 g
so 1 C m^{-2} loses 400 J g^{-1} = 4×10^9 erg g^{-1}
and 1 C m^{-2} is equivalent to 40 Mrad, an extremely high radiation dose.

This relation will hold for a range of specimen thicknesses, between 0.1 and 20 μm. Too thick specimens will reduce the average energy of the primary beam (to 90 kV at 25 μm) and so the energy loss rate will not be uniform throughout the specimen. Too thin specimens will allow some of the energy lost by the primary beam to escape. The amount of energy absorbed, and thus the dose, is then reduced. The energy will be carried away by fast secondary electrons, and also by X-rays and displaced atoms.

The escape due to secondary electrons can be estimated, assuming that the secondaries have an isotropic distribution and straight paths. Using energy loss rate tables [53] the average energy absorbed by a specimen of given thickness is estimated geometrically for each secondary energy above 50 eV. Lower energy electrons are assumed not to escape. The average energy loss, and the average energy absorbed are then calculated for these higher energy transfer collisions, allowing for the energy deposited at the primary event, 30 eV, say. The averages are weighted according to the probability of formation of a secondary of given energy. For 100 kV electrons passing through a foil of organic material, density 1 g cm^{-3}, the average energy loss, of losses over 80 eV, is 320 eV. If the foil is 10 nm thick, the average absorbed energy from these collisions is 110 eV.

The overall ratio of energy absorbed to energy lost depends on the fraction of energy transfers below 80 eV. This can be estimated from their mean energy, about 35 eV [55, 56] and the overall mean energy loss, about 80 eV [25, 57, 58] to be $(320-80)/(320-35) = 0.84$. Thus the average energy absorbed is $0.84 \times 35 + 0.16 \times 110 = 47$ eV, and only 60% of the energy lost by the primary beam is absorbed by the specimen. 1 C m^{-2} would then be equivalent to 25 Mrad instead of 40 Mrad. This result is in good agreement with the estimate that half the energy lost by an ionizing particle is deposited within 10 nm of its path [38].

Of course, the assumptions used are seriously in error, but the errors do act in opposing directions. Thus low energy secondaries are produced at nearly right angles to the primary beam, so that if the specimen plane is normal to the beam, as it usually is, the number which escape has been overestimated. However, the paths of low energy electrons are far from straight, so the effect of an initially anisotropic distribution will be much reduced. Curved paths will in themselves increase the numbers escaping, since electrons can be scattered out of the specimen, but not in.

This effect of specimen size will be very important for extremely thin, ultra-high resolution specimens [45, 15] but normally the value of 40 Mrad for 1 C m^{-2} at 100 kV is adequate as it indicates the extraordinarily high doses quickly received by a specimen in the electron microscope. The beam current density at a specimen in the electron microscope can be adjusted between zero and 10^5 A m^{-2}, using normal operating controls (bias, condenser lenses and apertures) but operating conditions normally lie within the range 10^{-1} to 10^4 A m^{-2}. Thus the dose rate varies between 4 and 400 000 Mrad sec^{-1}. This whole range corresponds to extremely high dose rates and the doses they lead to in usual microscope operation are correspondingly extreme. For example, it is well known that the crystallinity in polymers is destroyed in the course of usual electron microscopy. For polyethylene single crystals this destruction dose at room temperature is about 100 C m^{-2} at 100 kV, i.e. about 4000 Mrad. This dose can be obtained by irradiating for:

0.01 sec in E.M. at high beam current
20 min in E.M. at low beam current
5 weeks inside nuclear pile
1 year 0·5 m from 1 kCi ^{60}Co γ ray source
or by exploding a 10 MT H-bomb about 30 yards away.

In papers on electron microscopy, this same dose has often been described as "low", since when observing polyethylene special care is required not to exceed it [59] and since changes are

observed at doses 100 times greater. For example copper phthalocyanine crystals are destroyed at 3×10^4 C m^{-2} or 10^{12} rad [60] and the thermal and electrical conductivities of polystyrene and collodion are still changing at this dose [61, 62]. The very high dose rates given above refer to irradiation of a small area in the specimen plane. The electron microscope has been used [63, 64] to irradiate larger pieces of material placed in the viewing chamber or plate camera, where the maximum obtainable dose rate is inversely proportional to the area irradiated.

Radiation doses in the scanning transmission electron microscope should be similar to those in the conventional transmission microscope for similar resolutions. Since the image is formed by sequentially illuminating 10^6 picture points, the instantaneous dose rate during the pulse will be correspondingly higher, up to 10^{12} rad sec^{-1}. Such dose rates have been used in biological studies, though up to a total dose of only 10^5 rad [65] and no specific effects were attributed to the dose rate. The effect of irradiating in repeated micro-second pulses instead of continuously is otherwise unknown. In the ordinary SEM, with a specimen thicker than the range of the electrons in the beam, the situation is more complex, as the energy loss rate and thus the dose varies with depth. The heavy metal coating which is normal for non-conducting specimens will absorb some of the energy, and bring the region of maximum dose nearer to the surface. Studies of the effect of machine variables on radiation damage in the SEM have been made for crystalline polyoxymethylene (POM) [66] and amorphous polymethylmethacrylate [PMMA] polycarbonate and polystyrene [67]. The effects observed are very sensitive to the beam voltage and to the thickness of the evaporated gold coating used. POM and PMMA undergo scission and evolve gas, and these two materials were much more sensitive than the others used, in agreement with results from radiation chemistry [14] and transmission microscopy. In PE, similar damage has been observed in the transmission and scanning electron microscope [68] but no rate measurements were made to allow comparison of viewing times at similar resolutions.

4. Direct effects of radiation in the electron microscope

The detailed chemical and physical changes which occur in bulk polymers on irradiation cannot in general be observed in the electron microscope, simply because the irradiated mass is so small. Only three effects are directly observed, but each in itself can be sufficient to cause very great changes in the image formed in the microscope.

4.1. Loss of mass

Any bond breaking process, either main chain scission or side group loss, produces lower molecular weight species, and since the specimen in the electron microscope is very thin and in a high vacuum, some of these products will rapidly diffuse to the surface and evaporate. Thus the effect of scission is loss of mass from the specimen and hence increased transmission of the electron beam. Increase of transmission during observation in the electron microscope is indeed observed for almost all organic specimens, and it was one of the first radiation damage effects on polymers to be measured [69-72]. The increased transmission may be advantageous at times [e.g. 73] but it is preferable to use initially thin specimens if possible. Transmittivity of Formvar films has been more recently measured as a function of incident flux and beam voltage in an attempt to provide a specimen thickness calibration [74]. Mass loss has been observed in individual particles of polymer [75] and loss from biological specimens has been measured by autoradiography [76]. This takes time, but gives information about the loss of a particular element, the one which is radioactively labelled. Changes of elemental composition can be followed in this way. Change of mass and composition of polymers and biological materials have been studied in a specially constructed electron microscope analogue, where specimens large enough for chemical analysis can be irradiated [77, 78]. Using 75 kV electrons, and a low dose rate, these authors found that the specimens of several different types approached a steady state at doses of 100 to 1000 C m^{-2}. This final steady state generally contained proportionately more carbon and nitrogen than the original material and less oxygen, hydrogen and halides.

As a steady state is reached, the rates of opposing processes must become more and more similar. The rate of cross-linking must approach the rate of scission, the rate of unsaturation must approach the rate of hydrogenation. The actual processes occurring are unknown but one can see in very general terms how this situation may

arise after very large doses. For example, if cross-linking dominates initially, as in PE, a heavily cross-linked network forms, where the chains are more and more firmly held. As their motions are more restricted, chains are less likely to be able to come together and cross-link, unless a break occurs elsewhere. On the other hand, if the original material undergoes scission, as does collodion or POM, those parts most susceptible are affected most, and are removed from the material. If the remaining parts cannot cross-link at all, then the steady state produced would be when all the mass was lost. Experimentally, at least a few per cent is always left, so some of the new structures formed on irradiation must be of the cross-linking type, and material is lost until equilibrium is reached.

4.2. Loss of crystallinity

All the chemical changes produced by radiation, but particularly cross-linking, affect the intermolecular spacing of the polymer. If it is already amorphous, the diffraction rings corresponding to intermolecular spacings change their position [79]. If the material is ordered, then that order is lost. An oriented thin film of PE quickly loses its crystalline order, although the layer lines, corresponding to *intra*molecular spacings along the chain, persist for much longer [80]. When a polymer single crystal (Fig. 1) is the

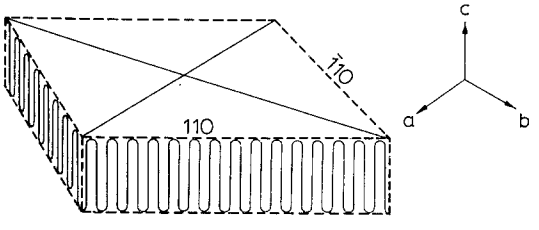

Figure 1 Highly schematic diagram of a polymer single crystal showing that an electric beam perpendicular to the plane of the crystal will be diffracted by intermolecular spacings.

specimens all the reflection observed are $(h,k,0)$ i.e. intermolecular, and the effect of radiation damage is dramatic (Fig. 2). The diffracted intensity diminishes, the spots may shift and broaden. The end result is a pattern of one or two diffuse rings. Detailed study of this process gives information about the type of structural changes being produced.

Orth and Fischer [50] showed that the diffraction spots from paraffin and POM single crystals remain sharp and stationary, merely fading away. This indicates disorder similar to thermal displacement, where long range order is undisturbed. PE is quite different, although chemically it is only high molecular weight paraffin. The spots shift and broaden, and the dependence of the width on diffraction order suggests a lattice distortion where the lattice vectors vary in magnitude and direction [50, 81] Kiho and Ingram [51] found that a combination of heat and irradiation produces a hexagonal form of PE.

The diffracted intensity from naphthacene, and from paraffin at low temperature, remains constant for an initial "latent dose" before decaying, but the intensity from paraffin at room temperature decayed exponentially [82, 83] with the same numerical decay constant found for the exponential decay from PE [84]. These authors emphasized the variable nature of the initial part of the intensity versus dose curve, but others [50, 85] have described an invariable decay for PE which has an initially constant part. Siegel [83] interprets his results in terms of target theory, but uses a "target" of one molecule, which would imply a molecular weight dependence of radiation damage, certainly not observed between paraffin and PE.

Many other authors have used the changing diffraction pattern as a reproducible measure of the progress of radiation damage, to observe the effect of variables such as specimen temperature. Heating polymer crystals always causes an increased rate of damage [50, 51, 80, 86]. The effect of cooling depends on the specimen itself. Materials which undergo scission, in particular POM [84] and L-valine and adenosine [87] are unaffected by cooling. Materials which cross-link damage at a slower rate when cooled, for although some authors find little difference is caused by cooling PE crystals [80, 88] Grubb and Groves [84] report a three fold improvement at 18 K and Siegel [82, 83] a five-fold improvement on cooling paraffin crystals to 4 K (also no increased transmission, i.e. no loss of mass at this temperature). A significant improvement is also found on cooling cellulose [89, 90] and phthalocyanine crystals [40].

These results agree with those of radiation chemistry, for example those of Geymer [21] mentioned in Section 2, where scission in polypropylene occurred on low temperature

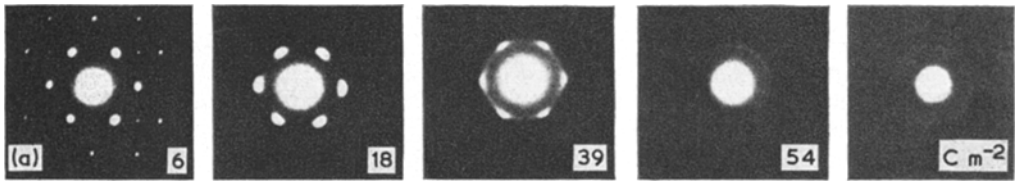

Figure 2 (a) Electron diffraction patterns from a single crystal of polyethylene at 75 kV, taken at increasing doses of irradiation. Photographic sequences such as this were used by Kobayashi and Sakaoku [80] to measure the effect of altering the beam voltage and specimen temperature. (b) Electron diffraction pattern from a single crystal of polyethylene after heavy irradiation at 80 kV (Grubb, unpublished).

irradiation, but cross-linking did not until the specimen was warmed. The eventual damage of cooled specimens in the electron microscope is explained by the very high doses used. A very high concentration of radicals is built up so that trapping does not prevent interaction. The latent dose observed at low temperatures, which is extremely important for forming an image of the undamaged material presumably corresponds to the dose required to build up the concentration of radicals. An exactly analogous situation occurs in the electron microscopy of alkali-halides, where the damage mechanisms are much better understood [91].

Decay of diffraction patterns from polymer crystals has also been used to measure the effect of different primary beam voltages. Increasing the beam voltage from 100 kV decreases the rate of damage [80, 92] by a factor of 3 at 1 MV [93]. At beam voltages of between 30 and 120 kV, it is found that the rate of damage is approximately inversely proportional to the beam voltage [50, 84, 94] in agreement with theory. No threshold voltage below which there is no damage has been discovered. Using a scanning electron microscope in transmission [95] and reflection [66] rapid damage in POM has been observed at a beam voltage of 5 kV. The prediction of increased damage at low energies has also been confirmed by the self irradiation of tritiated polystyrene, where the decaying tririum produces electrons of <18 kV [96].

As crystallinity is lost and diffraction spots fade, all features in the image which depend on diffraction contrast fade too. This severely limits the time available for observation of the image, and so limits the useful magnification and resolution attainable. If more than one micrograph is required from the same area (e.g. for dislocation analysis, [97]) the limitations are even more severe. Most features, for example dislocation images and bend contours (Fig. 3),

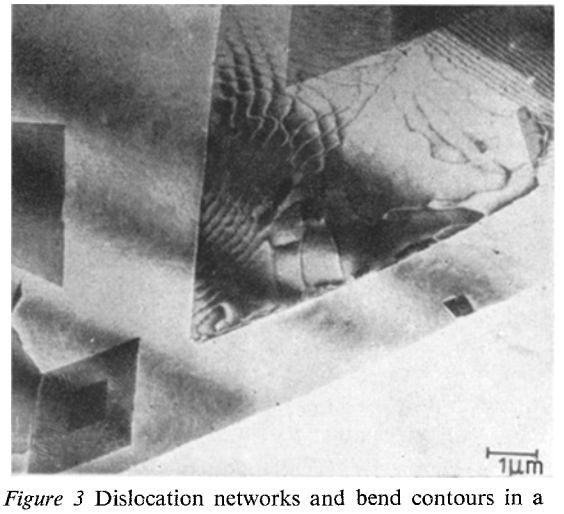

Figure 3 Dislocation networks and bend contours in a single crystal of low molecular weight polyethylene. Bright field electron micrograph from Sadler and Keller [179]. All of these features fade and disappear after a short period of irradiation.

will broaden as well as fade as the lattice directions become less well defined, and this will further reduce the possible resolution. Even in amorphous substances the structures visible in transmission through thin films [98] are rapidly affected by the beam so that only one useful micrograph can be obtained from a given area (Yeh, private communication).

Most calculations on attainable resolution (see Section 6) assume that the original contrast simply fades away to nothing, and nothing remains. In general this is not true, and other structures may appear temporarily or permanently during irradiation. The transient effects are diffraction contrast features which appear on irradiation, then fade away with the rest. In PE single crystals deposited on a carbon film, for example, the sequence of events which occurs is quite complex. The crystals were not originally flat; they were hollow pyramids, with a pyramid facet (sector) for each prism face. Because of this they are bent and tilted when they dry down onto the flat substrate, and no more than two of the four (1 1 0) sectors of the crystal can be in the correct orientation to diffract strongly (Fig. 4a). The others may have sharp bright bend contours on them, often at sector boundaries. These are artefacts caused by the bending and tilting which occurred when the crystal dried down to the substrate. On irradiation, the bend contours move about and broaden so that more of the crystal is bright. This is due to a combination of mechanical movement of the crystal and structural change within it, altering the lattice directions and making them less precise. A fine mottled structure, with regions 10 to 60 nm across then becomes visible, and very occasionally a more regular array of dark and light patches appears (Fig. 4b). The mechanism for this is unknown, but presumably local tilts appear as crystalline order breaks down, and this is compounded by mechanical instability of the crystal during irradiation. Regularity would require extremely uniform adhesion to the support film. The structure formed is superficially similar to that of the mosaic of 30 nm crystal blocks calculated from X-ray results [99] but the structure is *not* observed in undamaged crystals [100]. POM single crystals are almost flat originally, and simply fade away during irradiation. Even in this simple case, significant transient features can appear. For example, consider two crystals superimposed and slightly rotated to give a

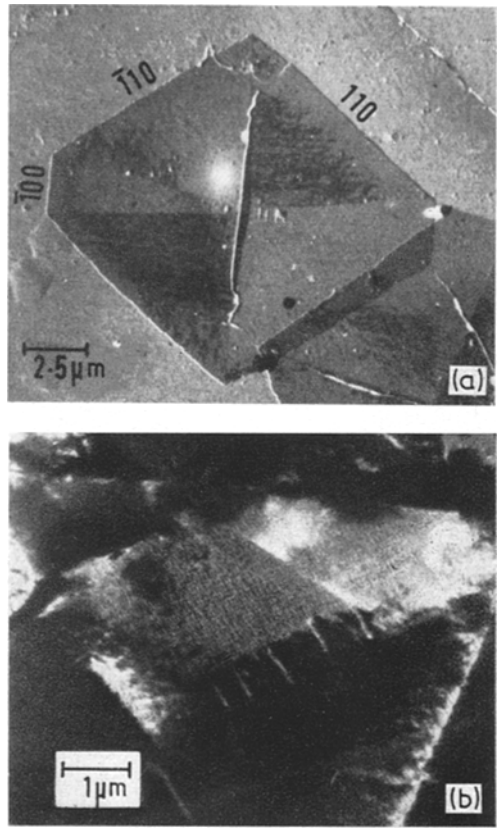

Figure 4 (a) Polyethylene single crystal in bright field. The 1 1 0 and $\bar{1}\bar{1}0$ sectors are diffracting and therefore, appear dark. The fine structure indicates local tilting perhaps because of irregularity of the support film. From Bassett and Keller [180]. (b) Detail of a polyethylene single crystal in 1 1 0 dark field after 20 C m^{-2} at 80 kV showing in one sector fine structure which appears during irradiation. Other bright features are the edges of the crystal, and wrinkles in a narrow 1 0 0 sector similar to those near the centre of the crystal in (a) (Grubb, unpublished).

Moiré pattern of parallel fringes. As the crystal becomes disordered and loses mass, its effective thickness is reduced, the lattice spikes in reciprocal space lengthen so that more reflections are excited. Thus the parallel fringes change into a hexagonal network. In melt-crystallized specimens, it is rare to be able to observe the diffraction contrast in any detail, let alone study its changes.

4.3. Contrast artefacts and distortion

The permanent contrast artefacts are much more important than the temporary artefacts described

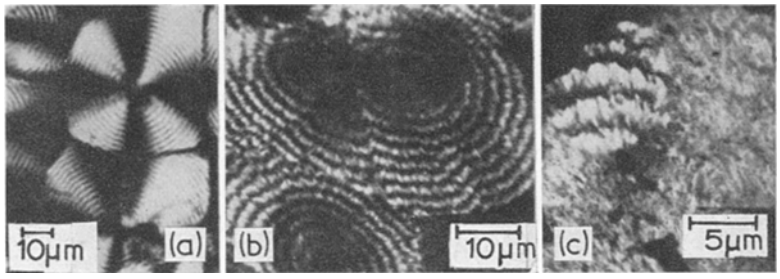

Figure 5 From Dlugosz and Keller [110]. (a) Optical micrograph taken with crossed polaroids of a section cut from bulk polyethylene. (b) Transmission electron micrograph of a thin section of the same material, taken after heavy irradiation. (c) The circular spot at upper left was heavily irradiated with a fine beam during focusing. The beam was then spread and the picture taken immediately.

above, simply because they are permanent. It is often difficult to see the fading crystallographic diffraction contrast features, even in crystals grown from solution, and the transient artefacts are merely an extra complication, but in specimens crystallized from the melt it is often extremely difficult to see anything *but* the permanent artefacts. At moderate beam currents necessary for viewing thicker specimens, the diffraction contrast from a polymer may be completely destroyed in a second, leaving only thickness contrast. The thickness contrast comprises the original mass thickness variation in the specimen, and thickness variations induced by radiation damage. Thus in an originally uniform specimen, the contrast visible after a second may all be an artefact, stable during further irradiation. It is hardly surprising that early investigators did not realize that rapid changes had taken place, particularly as the stable images observed were very much as expected.

To be more specific, thin films of PE were prepared which contained spherulites showing concentric dark and light bands in the polarizing optical microscope, superimposed on the characteristic maltese cross (Fig. 5a). X-ray diffraction results and the maltese cross imply that the spherulite is made up of crystals radiating from the centre. Careful and detailed optical microscopy of PE spherulites [101-104] showed (by tilting experiments) that the birefringent bands were produced by crystals twisting about the radial growth direction, and all twisting in phase (Fig. 6). Electron micrographs showed structures with concentric dark and light bands of the same periodicity as in the optical microscope, and in the dark bands twisted radial structures were visible [105, 106] (Fig. 5b). The structures are visible in the optical microscope because of their birefringence, and this cannot be a cause of contrast in the electron microscope. It was suggested [107] that the contrast was due to density differences between the crystalline and amorphous regions, somehow preserved during destruction of crystallinity. On this view, dark rings visible in the optical microscope were due to low crystallinity and it was necessary to postulate that the amorphous contrast varied cyclically along the spherulite radius, contradicting the results of optical microscopy. It was later thought that the contrast might be due to the thickness variations which were known to exist in the thin cast films used for electron microscopy [108] so the model of varying amorphous content was revived when similar contrast was seen in sections originally of uniform thickness [109]. However, Dlugosz and Keller showed in 1968 [110] that sectioned specimens of PE had no visible structure at first and the band structure became visible only on irradiation (Fig. 5c). This made it clear for the first time that the visible structure was a stable artefact, and that thickness variations were produced by irradiation.

The loss of mass on irradiation (Section 4.1) was well known, and it was natural to think of the contrast as being produced by some sort of differential etching. However, the contrast produced can be considerable and there is no reason for grossly different chemical effects to occur at different crystal orientations. It has been recently shown that the basic cause of the contrast is a change of shape, or distortion, of the basic crystalline units [1, 68, 111]. Some polymer crystals in the electron microscope tend to

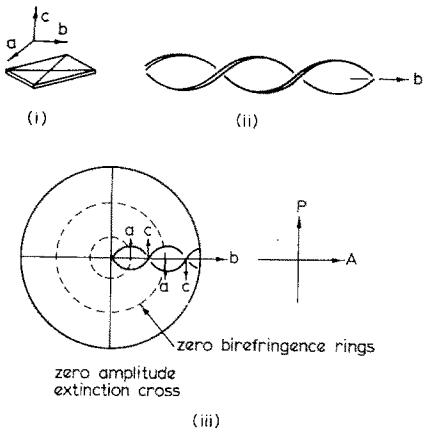

Figure 6 (i) The crystal axes of a polyethylene crystal. (ii) The twisted crystal ribbon which is the radial unit of the spherulite. (iii) P and A are the polarizer and analyser directions. The refractive indices of polyethylene in the *a* and *b* directions are almost equal, so that when *a* lies in the plane of observation there is no birefringence. The radial units, twisting in phase, give dark rings at these positions.

become smaller in one direction, and larger in others. When the first direction is parallel to the electron beam transmission through the specimen increases, and when the second directions are parallel to the electron beam transmission decreases. Thus a uniform film containing different crystal orientations becomes non- uniform, and concentric thick and thin bands are formed in a spherulite.

The change of shape of single crystals on irradiation in the electron microscope was not observed for many years, because the most stable substrate was chosen, an amorphous carbon film. PE crystals irradiated on a carbon support film seem quite stable. A slight doming occurs, which is only visible if the specimen is shadowed after irradiation [111]. However, the stability is conferred by the strong and rigid carbon film, and is not a property of PE. If the crystal is supported by a soft collodion film which allows motion, it expands in the plane of the support film, by over 50% in area, equally in all directions [111]. Since the mass of the crystal is only slightly reduced by irradiation, the mass thickness is reduced to 62% of its original value. The density of PE tends to rise on irradiation [30, 112] so the actual thickness must also be reduced by this much. The thin lamellar crystal contracts parallel to *c*, the chain direction, and becomes even thinner; at the same time it expands perpendicular to *c* and becomes wider. When such a crystal lies flat on a collodion film, the film is pushed back, spread out and made thinner locally by the expanding crystal so that the contrast of the specimen reverses (Fig. 7).

Before going on to describe the detailed predictions and experimental agreement for this model in the case of PE, it must be pointed out that the effect is general. In all cases where a permanently visible structure appears in the electron microscopy of pure unstained melt-crystallized polymers, it is a radiation artefact caused by crystal distortion. Thus Andrews observed in 1962 [113] great changes in spherulitic thin films of natural rubber during irradiation in the electron microscope. Areas which were originally dark and gave a single crystal type of diffraction pattern with the chain direction parallel to the beam, became much lighter after irradiation. Radiating fibrils appeared in other areas, which got generally darker. At the same time, the film tended to contract, but the single crystal areas did not, and the shape of the spherulite changed, becoming conical. The explanation given by the author was in terms of crystalline and amorphous regions rather than crystals at different orientations. Thin cast films of poly-4-methylpentene-1 reverse their contrast in the beam, and the structures observed are quite similar to those in rubber. Single crystals of this material, like those of PE, appear stable on a carbon support film, but on colodion expand in their own plane, by 15% in area (Grubb, unpublished). Thin films of nylon have lasting contrast features in the electron microscope [114, 115] and it was found that the contrast was produced during irradiation, and depended on the crystal orientation; regions

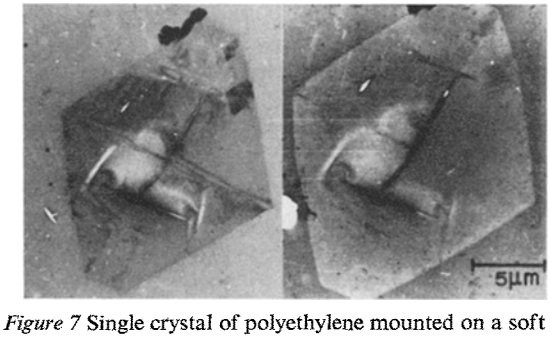

Figure 7 Single crystal of polyethylene mounted on a soft support film before and after irradiation. Bend contours disappear, the crystal expands and contrast reverses: after Grubb *et al.* [111].

with the *c*-axis parallel to the beam became lighter (1963, Harris, private communication). Ultramicrotomed sections of Nylon 66 increase their contrast from nothing in the beam [116], but there is so far no information on single crystal distortion. Khoury [117] saw anisotropic deformation of polypropylene quadrites, which are aggregates of lamellar crystals grown from solution. These aggregates were only loosely attached to the substrate film in the electron microscope. Six years later increasing contrast in polypropylene sections has been observed [118]. Solution grown single crystals of POM do not expand on irradiation, they merely become thinner, but thin films of POM have little contrast after irradiation [95].

In each case thin films undergo contrast reversal, but the contrast of cut sections increases. The difference is only due to the greater thickness of the sections which obscures the initial diffraction contrast, and not to any difference in fundamental properties. More recent, thinner, ultramicrotome sections of PE show strong initial diffraction contrast, and contrast reversal during irradiation (Dlugosz, unpublished). In thin specimens, the regions initially dark in bright field, that is, those which diffract more electrons, are not more crystalline than the rest but better oriented for the excitation of the strong (*hk*0) reflections. Hence they are like deposited single crystals, lamellae flat-on in the film. On irradiation the coherent diffracting power is lost, and the lamellae expand laterally, becoming more transparent. Other regions, with the crystals edge-on, diffract weakly and on irradiation the lamellae expand parallel to the electron beam, giving a dark region. Lamellae in this position will be distinct and visible [108].

The distortion of crystalline sub-units produces not only contrast, but also distortion of the whole specimen. In the case of PE good quantitative agreement exists between the distortion in single crystals and that in spherulites, even though the exact constraints operating in each case are not known. The crystals of a PE spherulite have their *b* direction radial, and as the crystals twist the *a* and *c* directions rotate about *b* (Fig. 6). Single crystals on irradiation expand by 23% along *a* and *b* and contract by 38% along *c*. Therefore, the radii of spherulites in a thin film should expand to 1.23 of their original value, and the average thickness and circumference should contract to $(1.23 \times 0.62) = 0.88$. The thickness is free to contract, but the circumference and radius are geometrically linked, and the only way to accommodate both changes is for the spherulites to become right circular cones, with semi-angle $\sin^{-1}(0.88/1.23) = 46°$. Spherulites of PE do become conical in the electron microscope, with a semi angle of $45 \pm 3°$ [68], and spherulites of rubber [113] and polystyrene [119] also become cones. When slices of bulk-crystallized polymer are used, the spherulites will probably be cut in off-diametral sections, so that at the apparent centre, the radial direction, and the lamellae, are vertical, perpendicular to the section plane. This modifies the predicted cone to a dome, or spherical cap, and domes are observed [109]. The three dimensional structures produced are most clearly seen in the scanning electron microscope [1, 68, 120] (Fig. 8). The flat regions at the borders of the spherulites are caused by the constraint of surrounding unirradiated material. Their presence, and the sudden change to an unaffected cone, are predicted by the model [68]. A thick specimen will only be irradiated to the penetration depth of the electrons, and the unirradiated material will further limit the movement of the irradiated surface. Breedon *et al.* [120] use the artefacts seen to derive an altered model for PE spherulite structure, where the lamellae do not twist completely, but the identification of the bumps seen with lamellar units is not certain.

Spherulites are complicated, simpler arrangements of crystals distort in a simpler way. Thus holes in a thin film nucleate a large number of "edge-on" lamellae which grow radially out from the hole, and when the film is irradiated, such holes contract [113]. Oriented structures produced by drawing contract considerably in the electron microscope, but it is difficult here to separate distortion from relaxation.

It may seem odd that a lamellar crystal, already much thinner in one direction than in any other, becomes even thinner in that direction as it loses its order. However, within the crystals the molecular chains run parallel to the thinnest dimension (Fig. 9a). Except at the surfaces where they fold back into the crystal, they are fully extended. Hence any disordering of the orientation in the crystal must reduce the end-to-end distance of the extended part, and thus the lamellar thickness (Fig. 9b). Unless the density rises, the width of the lamellae will increase.

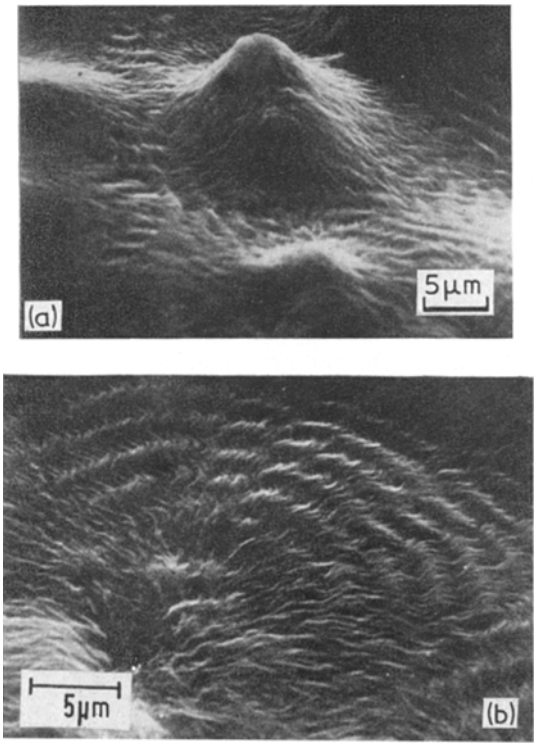

Figure 8 A thin film of polyethylene cast from solution, mounted on a copper grid and lightly coated with gold, observed in the scanning electron microscope at 20 kV (a) The area to the right has been exposed to the beam for some time, the smooth area to the left has not. The specimen is tilted forward by 60°, to show clearly the conical shape of the spherulite in the centre of the picture. (b) This unusually flat area is tilted by 45°, and shows more clearly the radiating fibrils, all in phase over small sectors separated by faulted regions.

Cross-linking introduces disorder of chain orientation, even in its simplest schematic form (Fig. 9c) while chain scission may not. PE and the other polymers which show the permanent artefacts described all cross-link. Polymers which undergo scission are general featureless after irradiation, unless they are stained, though some structures are produced in POM [66].

With the knowledge of how the artefacts form, one can work back from the micrographs taken after irradiation to the original structure with much more confidence, and this is very necessary because it may be difficult or impossible to resolve the undamaged structure directly (see Section 6).

5. Secondary effects of the electron beam

5.1. Heating

When gross changes in organic materials are observed in the EM, it is natural to attribute them first to heat, because the temperatures required to produce such changes are within the range of ordinary experience, and the radiation doses required are definitely not. It is difficult to appreciate that because of the small size of the irradiated area, an enormous irradiation dose rate may produce a negligible temperature rise, but such is the case. We know that the heating effect can be kept small simply because low melting point (40 to 50°C) crystals can be observed without melting them [121]. On the other hand, it is easy to produce high temperatures with the beam of a TEM, either intentionally or unintentionally, and Yamaguchi [122] claims that paraffins can be melted (at 70°C) by the beam without significant radiation damage.

The temperature rise will depend on the rate of energy absorption (Section 3) and on the rate of energy dissipation, i.e. on the thermal conductivity of the specimen, the area irradiated, the distance to a good conductor, thermal contact of specimen to grid and grid to holder. Heating or cooling devices will, of course, affect the specimen temperature directly. The temperature rise for a thin uniform film in perfect contact with its surroundings has been calculated by many authors [62, 86, 123-128]. Although the calculations are for an ideal situation, the available experimental evidence, limited by the difficulty of measuring the true specimen temperature [126, 129, 130], does support the theoretical conclusions. Thermal radiation is normally negligible compared to conduction, so the maximum temperature rise is proportional to the beam current. For an organic specimen mounted on a 200 mesh grid, the constant of proportionality at 100 kV is approximately 3°C nA^{-1}. With a 20 μm diameter spot and current density of 10 A m^{-2}, the current is 3 nA so the rise in temperature at the centre of the illuminated area will be 9°C. Thus with the beam current density range described above, 10^{-1} to 10^{4} A m^{-2}, the temperature rise varies from the negligible, 0.09°C to the catastrophic 9000°C.

It has been suggested that allowing the beam to touch the supporting grid will cause a large temperature rise, and must be avoided [80]. This is not so, because the comparatively thick

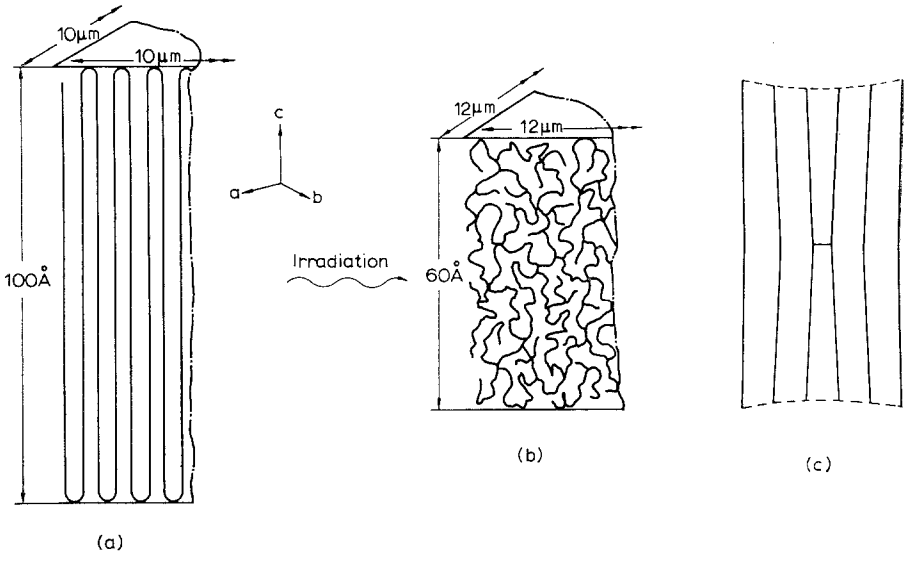

Figure 9 A schematic drawing showing a corner of a solution grown polyethylene single crystal (a) in its normal state before irradiation; (b) after intense irradiation, with the chains randomized. The deformation shown occurs when a collodion substrate is used; (c) Schematic drawing of a cross-link in an otherwise perfect lattice (after Kobayashi and Sakaoku [80]) showing that the crystal thickness must be reduced.

copper is such a good conductor of heat that whatever fraction of the incident beam energy it absorbs, its temperature rise will be much less than that of the thin specimen. It is true that when the grid is exposed to the beam, the specimen and grid will absorb more energy. However, the previous calculations assumed, pessimistically, that the illuminated spot was in the middle of a grid square. If it is adjacent to a grid bar the temperature rise with respect to the grid is less, so the total rise may not be greater, as Reimer and Christenhusz [62], and Stenn and Bahr [15] infer. In any case the effect will be very much less than that of poor thermal contact with the grid, or simply increasing the beam current. Thus direct damage by heating is likely in the TEM only when high beam currents are used to penetrate thick specimens [e.g. 131, 132] and even then the most common gross damage, bubble formation, may be due to the trapping of gaseous products which normally diffuse out of a thin specimen, rather than to the temperature rise.

Similar calculations for the SEM show that the temperature rise for a given beam current is much less than in the TEM, simply because the heat can be conducted away in three dimensions instead of two. A deliberate attempt to melt polymer samples in the SEM, using high beam currents and a stationary beam, failed completely (Arrowsmith, private communication 1971). When the beam is scanning, the situation is complicated, but the temperature rise must be less.

When damage by heating does occur, it can be recognized for what it is, because the effects of heat and irradiation on organic materials are different [80, 133-136].

A temperature rise which is of no importance in itself can have an important effect through the temperature dependence of radiation damage. In general the chemical yield of radiation increases as the temperature increases, so the rate of damage should also increase. This has been experimentally verified for polymer crystals [50, 51, 80, 121]. Since the electron beam produces a temperature rise which depends on beam current, the same dose should give a greater effect if it is applied at a greater rate. When measurements have been made, some workers find a dose-rate dependence [60, 71, 94, 128] and others find that dose rate has no effect [80, 84, 87, 115, 137]. The contradiction is only apparent, not real, because the former group used high dose rates, and the latter low dose rates, generally below 1 A m^{-2}. A dose rate of 1 A m^{-2} would produce a temperature rise of about 1°C under the typical conditions described above, where 10 A m^{-2} gives a 9°C rise. Interpolating from the results of Orth and Fischer [50] (as in [84], Fig. 7) a

rise of 1°C affects the damage rate of PE single crystals by 3%, a rise of 9°C by 28%. The accuracy of measurement of damage effects is certainly no better than 5%, so at low dose rates the rate dependence cannot be observed.

An increase of temperature can also affect the final state of the specimen. It has been shown for several synthetic and natural polymers that the loss of mass in the EM is greater at higher beam intensities [60, 70, 72, 78] and induced contrast in PE is also greater [109]. These effects are observed at high beam current densities, where the temperature rise may be considerable, and are attributed to increased mobility within the specimen, although Stenn and Bahr [78] found that heating the specimen whilst irradiating at a low dose rate did not have the same effect as irradiating at a high dose rate.

5.2. Electrostatic charging

In the TEM, a thin specimen absorbs no primary electrons, but secondaries are emitted, so a positive charge builds up. The statistical nature of the process involved produces large, rapidly varying fields within a poorly conducting specimen. These can affect the image, to give the impression of rapid fine scale movements in the sample when it is slightly out of focus [138]. Fields of up to 10^6 V m^{-1}, comparable to the breakdown field for dielectrics, can be produced [139]. Such fields could affect chemical reactions, and it has been suggested that electrostatic effects are the important factor in beam damage [140, 141]. Recent experiments have shown that an organic molecular crystal is damaged more slowly by the beam when it is coated with gold on both sides [142], and the mass loss from a biological section is reduced by coating with aluminium. The protection given may be due to the increased electrical or thermal conductivity of the sample, or the metal may act as a trap for excitations in the organic material, or the coating may simply prevent evaporation of fragments, increasing the cage effect and the probability of recombination. More experiments will be necessary to distinguish between these possibilities.

An overall charge can also build up on the specimen, which can distort the image and the repulsive forces can fragment the specimen. The effect is greater when the objective aperture is removed. With extremely thin PE films, it is common to have a stable undistorted bright-field image, but on going to diffraction conditions, the beam is deflected and the specimen breaks up. Apparently electrons scattered from the aperture and its holder back up to the specimen help to neutralize its positive charge. The charging effect is not as important as might be expected, because the conductivity of most organic materials is enhanced by radiation [60, 14 p. 348, 143].

Overall charging causing disturbance of the image is better known in the scanning electron microscope. There thick specimens do absorb primary electrons and normally the secondary electron emission coefficient σ is less than 1 so that negative charge builds up on non-conducting specimens. The normal solution to this problem is to coat the surface to be examined with metal by evaporation. A thick metal layer would prevent radiation damage, by stopping the electrons before they reach the material, but coatings normally used are much too thin to do this. Alternative solutions are to use a very low beam voltage of around 2 kV, where $\sigma \simeq 1$, but the resolution obtainable is not good, or to spray the specimen with 1 kV electrons from a separate electron gun during the fly-back time of the imaging beam, and adjust the current so that the average value of σ is 1 [144]. The low energy electrons will cause severe damage, but only to an extremely thin surface layer.

5.3. Influence of the surrounding atmosphere

The atmosphere in an electron microscope is normally a vacuum of 10^{-4} Torr or less, and this in itself is sufficient to cause severe damage to many organic specimens. Biological materials lose water, and low molecular weight materials may simply evaporate. Synthetic polymers are normally unaffected by vacuum, although a complex formed with a low molecular weight material can be affected [145, 146], but they are not immune to the effects of residual gases. When, as is usual, the residual gases are largely hydrocarbons, they cross-link in the beam while absorbed on the specimen, and carbonaceous material builds up. This is contamination [147, 148]. If water vapour is the main constituent, it is dissociated by the beam while absorbed and the result is oxidation and removal of material from the specimen [149]. Loss of carbonaceous material also occurs in low pressure oxygen environments [150]. Like all radiation damage effects, these increase in rate with beam current density and are more important at high resolution. Hence at the low magnifications often used

for polymers because of direct radiation damage, contamination is negligible when a cold finger anti-contamination device [151] is used. On the other hand, Siegel [152, 153] has considered it necessary to build a U.H.V. system to reduce contamination sufficiently for atomic resolution.

6. Resolution obtainable

6.1. Statistical limit

Radiation damage causes there to be a limit to attainable resolution, because at low doses the statistical fluctuations of intensity may obscure the image, and at high doses the structure is destroyed. Under given conditions, the structure will be destroyed after a specific number of electrons per unit area, J, have passed through it. If a square of side d is to be resolved containing a feature of contrast c, and if f is the fraction of electrons passing through the specimen which contribute to the image, then the number of electrons which can form an image of this square is Jd^2f, the signal produced is Jd^2fc and the statistical noise is $(Jd^2f)^{\frac{1}{2}}$. The signal-to-noise ratio is $Jd^2fc/(Jd^2f)^{\frac{1}{2}}$. If there is a minimum acceptable signal-to-noise ratio for visibility, k, then the object can just be resolved when

$$k = (Jd^2f)^{\frac{1}{2}}c \quad \text{i.e. } d = k/c(Jf)^{\frac{1}{2}} \quad [154, 137]. \quad (1)$$

There is considerable uncertainty over the precise values which should be chosen for the various factors, so the value arrived at for d may not be very reliable. Values for k from 3 for a periodic image to 50 for a good quality image have been used, but the commonest by far is 5. The test plates originally used to establish this figure [155] consisted of circles arranged in rows and columns of increasing noise. For an unknown disordered specimen, a much higher value might be appropriate. Defining c, the contrast, needs a precise description of the structure to be resolved and the conditions of viewing. For f, the collection efficiency of the image, the method of formation of the image, (dark or bright field, or annular aperture) and the aperture sizes are among the variables.

Further, the assumption that the structure remains perfect up to a critical dose J after which it is useless is too simple. It is best to assume that the contrast of the structure falls with irradiation in the same way that diffracted intensity falls, and then calculate the optimum dose beyond which the statistics do not improve. Even then the calculation is only valid if the feature does not shift, broaden or relax. The best possible resolution in PE at 100 kV has been calculated to be 0.5 nm [95] for the specific case of a rotation Moiré pattern formed between two crystal layers each 12 nm thick, assuming that the initial contrast was as given by the two beam kinematic approximation [156] and that a signal-to-noise ratio of 3 was sufficient. This is definitely an idealized situation, and the best published resolution under very similar conditions has been 4 nm [59]. No allowance was made for the time required to focus the image, but it is standard practice to focus elsewhere and move either the specimen or the beam to irradiate a new area just before taking a micrograph. Thomas and Ast [85] made allowance for focusing and found that using an image intensifier then gave a considerable advantage. With the resolved structure being a small area of PE single crystal 12 nm thick, diffracting strongly into a (1 1 0) reflection and surrounded by similar material which is not diffracting, they arrived at 5 nm resolution at 100 kV. Glaeser [137] has made similar calculations for single crystals of biologically important materials, with a square of diffracting crystal as the object to be resolved, but with no allowance for focusing. He obtains 5 nm for L-valine and 2 nm for adenosine. The calculation broke down on stained catalase, because the resolution calculated from the decay of the strong inner diffraction spots, which arose from spacings of 9 nm, was only 0.16 nm, although the spots from spacings <1 nm had disappeared much earlier, indicating disruption of the fine structure. This makes it clear that when using the decay of diffracted intensity as a measure of degradation, one must use reflections corresponding to spacings less than or equal to the resolution obtained. Normally the innermost reflections come from spacings of about 0.4 nm, so the point does not arise. Whatever the accuracy of these individual estimates the important point is that for this class of specimens radiation damage is the limiting factor, and resolution of the original structure will, in practice, be affected by alterations in the variables of Equation 1.

6.2. Improving resolution

From Equation 1, one way of improving the resolution (reducing d) is to delay the appearance of radiation damage (increase J), and from the results quoted in Section 4.2 it would appear that operation at higher beam voltages would increase J for all organic materials by reducing the

radiation dose per electron. However, the diffracted intensity from a thin specimen falls at high voltages so that contrast c (in bright field) or efficiency f (in dark field) is diminished, and this reduces the improvement. The advantage gained may be further whittled away in practical terms as the screen resolution [157] and photographic efficiency [158, 159] are generally poorer at very high voltages. The loss of photographic efficiency is not important when the time required for focusing is taken into account [58]. Thomas and Ast have gone into this point in detail for a PE single crystal specimen. They find that when an image intensifier is used, or when focusing is done on one area and recording from an adjacent area, optimum resolution can be obtained at any beam voltage between 50 and 300 kV. They predict that when the same area is used for focusing and recording, without an image intensifier, 300 kV is best, in agreement with an earlier qualitative estimate [160].

Cooling to liquid nitrogen or liquid helium temperatures should improve the resolution limit for some but not all specimens. The advantage is to be gained not only from an increase in J but also from the appearance of an initial latent dose when the specimen is relatively stable. The improvement can only be realized if the cooling stage does not reduce the convenience and rapidity of operation of the microscope. Cooling and high voltage operation should improve matters not only for crystalline materials but also for partially crystalline and amorphous materials which are radiation sensitive.

One may also improve the resolution by improving the contrast, c, or efficiency f. These two are often linked, so the important factor is $cf^{\frac{1}{2}}$ which appears in Equation 1. Contrast from a crystalline material is affected by the orientation and the reflection used to form the images but these variables are normally fixed by other considerations. The contrast of partially or wholly amorphous material may be increased by staining, which is commonly used in biological specimens, but rarely in synthetic polymers [2, 161, 162]. The stain will have a self structure, limiting resolution, but this limit is not normally reached. The stain may confer stability on the specimen, but it need not do so. For example, stained collagen fibres split and perforate in the electron beam [163, 164]. Contrast may be enhanced by altering the operating conditions of the microscope. An annular aperture [165, 166] or phase plate [167] will give a larger $cf^{\frac{1}{2}}$ than either bright- or dark-field operation.

The minimum acceptable signal-to-noise ratio, k, will be smaller if the structure is repeating and easy to recognize, and this will improve the resolution. It may be improved much more if the repeating units are superposed to give an image of the average unit. Further improvements can be achieved by more complex image processing [168].

The efficiency of the recording medium should be taken into account when calculating the statistical limit, but this can be ignored normally, because most photographic emulsions are very efficient detectors of electrons at ordinary electron microscope voltages [169]. Their response to electrons has been studied in detail [170, 171] and is very different to their response to light. The optical density of the processed emulsion is proportional to electron exposure, so that all emulsions have the same contrast which increases with exposure [170]. Since the statistical resolution limit (Equation 1) is intrinsic to the signal, the resolution is unaffected by the speed of the emulsion. A fast emulsion can be used at higher magnification, but since the exposure is less, the noise is greater and referred back to the specimen there is no difference. There may be some difference in practice, in that a slow plate used at a very low magnification may not be able to resolve the detail because of electron diffusion within the emulsion [170] and it may be much easier at a higher magnification to use the electron microscope, and to focus the larger but fainter image. This may be the reason for the differences noted by Matricardi *et al.* [159] who find that fast plates are better.

Since the photographic plates (and films) are efficient detectors no kind of image intensifier or TV system [172-174] can improve on their resolution, at best they can equal it. However, intensifiers can be very useful in providing a bright though noisy image for finding an interesting area and setting up the picture before recording it photographically. One can gain by using an intensifier to focus [174] and this is because the eye and brain can interpolate the position of optimum focus for detail several times finer than that contained in the image viewed. Many commercial image intensifiers are extremely expensive, so a cheap system [175] is of great interest, especially since it has been found

that dark adapting the eye for half an hour has an excellent "intensification" effect [176]. Most electron microscope rooms are far from dark, and modern microscopes are covered with indicator lamps that normally prevent dark adaptation.

So far it has been assumed that the statistical limit described by Equation 1 is the limit to all information obtainable from the specimen. This is not so, because the permanent artefacts described in Section 4.3 give information on the structure of the specimen, and can continue to do so for an unlimited time. The particular artefacts described for PE do not affect the resolution limit because they are all large scale effects, thickness changes of up to 100 nm and motions of several microns being involved. It was only possible to interpret the images and describe the process of damage leading to these artefacts because of their large scale, since this allowed the original structures to be resolved in the optical microscope and in the electron microscope at low doses. If similar basic units, groups of well-oriented long chain molecules, are involved in fine scale structure, for example the structure claimed to exist in amorphous polymers [98] then the same type of artefact should occur. Knowing the cause of permanent contrast features in polymer specimens, it should be possible to obtain information about unknown structures from electron micrographs taken after radiation damage is complete. This is true whether or not the scale of the unknown structure is larger than the statistical resolution limit for diffraction (Equation 1). If the structure is of very fine scale, approaching the resolution limit of the microscope, very great care in interpretation will be required [177, 178].

Acknowledgements

I should like to thank Professor A. Keller for his continued assistance and the S.R.C. for financial support. This review is based on a short review which was given at the Fifth European Congress on Electron Microscopy, 1972, [1].

References

1. D. T. GRUBB and A. KELLER, Proceedings of the 5th European Congress on Electron Microscopy, Manchester (Institute of Physics, London and Bristol, 1972) p. 554.
2. R. C. WILLIAMS and H. W. FISCHER, *J. Molec. Biol.* **52** (1970) 121
3. K. KATO, *J. Polymer Sci.* **B4** (1966) 35.
4. D. PINES, *Rev. Mod. Phys.* **28** (1956) 184.
5. G. R. FREEMAN, *J. Chem. Phys.* **46** (1967) 2822.
6. J. K. THOMAS and R. V. BENSASSON, *ibid* **46** (1967) 4147.
7. T. J. HARDWICK, *Discuss. Faraday Soc.* **36** (1963) 267.
8. E. S. COPELAND, T. SANNER and A. PIHL, *Int. J. Radiat. Biol.* **18** (1970) 85.
9. E. COLLINSON, J. J. CONLEY and F. S. DAINTON, *Discuss. Faraday Soc.* **36** (1963) 153.
10. J. L. MAGEE, *ibid* **36** (1963) 232.
11. F. WILLIAMS, in "Fundamental Processes in Radiation Chemistry", edited by P. Ausloos (Interscience, New York, 1968) p. 518.
12. P. AUSLOOS, Ed., "Fundamental Processes in Radiation Chemistry" (Interscience, New York, 1968).
13. J. W. I. SPINK and R. J. WOODS, "An Introduction to Radiation Chemistry" (Wiley, New York, 1964).
14. A. CHAPIRO, "Radiation Chemistry of Polymeric Systems" (Interscience, New York, 1962).
15. K. STENN and G. F. BAHR, *J. Ultrastruct. Res.* **31** (1970) 526.
16. K. L. HALL, R. O. BOLT and J. G. CARROLL, in "Radiation Effects on Organic Materials" edited by R. O. Bolt and J. G. Carroll (Academic Press, New York, 1963).
17. R. H. PARTRIDGE, *J. Chem. Phys.* **52** (1970) 2485.
18. A. CHARLESBY, *Proc. Roy. Soc.* **A215** (1952) 817.
19. M. DOLE, C. D. KEELING and D. G. ROSE, *J. Amer. Chem. Soc.* **76** (1954) 4304.
20. A. N. PROVEDNIKOV, YIN-SHEN-KAN and S. S. MEDVEDEV, *Dokl. Akad. Nauk. SSSR* **122** (1958) 254.
21. D. O. GEYMER, *Makromolek. Chem.* **100** (1967) 186.
22. R. SALOVEY and A. KELLER, *Bell Syst. Tech. J.* **40** (1961) 1397.
23. T. KAWAI, A. KELLER, A. CHARLESBY and M. G. ORMEROD, *Phil. Mag.* **12** (1965) 657, see also following papers to p. 718.
24. G. N. PATEL, L. D'ILARIO, A. KELLER and E. MARTUSCELLI, *Makromolek. Chem.* **175** (1974) 983.
25. L. MANDELKERN, in "The Radiation Chemistry of Macromolecules", edited by M. Dole (Academic Press, New York and London, 1972).
26. P. ALEXANDER and R. M. CHARLESBY, *Proc. Roy. Soc.* **232** (1955) 31.
27. J. T. MORGAN, R. SHELDON and G. B. STAPLEDON, RPP/13 Rutherford High Energy Lab. Chilton Didcot, Berkshire, England (1969).
28. P. ALEXANDER, L. D. G. HAMILTON and K. A. STACEY, *Nature* **216** (1967) 1208.
29. R. P. KUSY and D. T. TURNER, *Macromolecules* **4** (1971) 3.
30. A. CHARLESBY and M. ROSS, *Proc. Roy. Soc.* **A217** (1953) 122.
31. A. CHARLESBY, *J. Polymer Sci.* **10** (1953) 201.

32. W. P. SLICHTER and E. R. MANDELL, *J. Phys. Chem.* **62** (1958) 234.
33. R. BLACKBURN, A. CHARLESBY and R. J. WOODS, *Eur. Polymer J.* **1** (1965) 161.
34. T. F. WILLIAMS, H. MATSUO and M. DOLE, *J. Amer. Chem. Soc.* **80** (1958) 2595.
35. P. ALEXANDER and A. CHARLESBY, *Nature* **173** (1954) 578.
36. V. V. VOEVODSKII and YU. N. MOLIN, *Radiat. Res* **17** (1962) 366.
37. E. J. HART and R. L. PLATZMANN, in "Mechanisms in Radiobiology", edited by M. Errara and A. Forseberg (Academic Press, New York, 1961).
38. B. PULLMAN and A. PULLMAN, "Quantum Biochemistry" (Interscience, New York, 1963).
39. J. W. MENTER, *Proc. Roy. Soc.* **A236** (1956) 115.
40. N. UYEDA, T. KOBAYASHI, M. OHARA, M. WATANABE, T. TAOKU and Y. HAWADA, Proceedings of the 5th European Congress on Electron Microscopy, Manchester (Institute of Physics London and Bristol, 1972) p. 566.
41. N. UYEDA, T. KOBAYASHI and E. SUITO, *J. Appl. Phys.* **43** (1972) 5181.
42. A. CHARLESBY, "Atomic Radiation and Polymers" (Pergamon, Oxford, 1960).
43. M. DOLE, Ed., "The Radiation Chemistry of Macromolecules" (Academic Press, New York and London, 1972).
44. G. J. DIENES and G. H. VINEYARD, "Radiation Effects in Solids" (Interscience, New York, 1957) Chapter 3.
45. V. E. COSSLETT, Proceedings of the 25th Anniversary Meeting of the Electron Microscopy and Analysis Group Cambridge (Institute of Physics, London and Bristol, 1971) p. 6.
46. A. CHARLESBY, A. R. GOULD and K. J. LEDBURY, *Proc. Roy. Soc.* **A277** (1964) 348.
47. D. T. GRUBB, *J. Phys. E; Sci. Instrum.* **4** (1971) 222.
48. L. H. BOLZ, D. H. RENEKER and K. W. YEE, *ibid* **5** (1972) 1039.
49. D. G. DRUMMOND, *ibid* **4** (1971) 247.
50. H. VON ORTH and E. W. FISCHER, *Makromolek. Chem.* **88** (1965) 188.
51. H. KIHO and P. INGRAM, *ibid* **118** (1968) 45.
52. H. A. BETHE, *Handbuch der Physik* **24(1)** (1933) p. 273 *et seq.*
53. D. E. LEA, "Actions of Radiation on Living Cells" 2nd Edn. (Cambridge University Press, London and New York, 1955).
54. W. LIPPERT, *Optik* **15** (1958) 293.
55. R. E. BURGE and D. L. MISELL, *Phil. Mag.* **18** (1968) 251.
56. D. L. MISELL and R. A. CRICK, *J. Phys. C* **2** (1969) 2290.
57. A. M. ROUTH and J. A. SIMPSON, *Radiat. Res.* **22** (1964) 643.
58. V. E. COSSLETT, *Berichte der Bunsen-Gesellschaft* **74** (1970) 1171.
59. A. W. AGAR, F. C. FRANK and A. KELLER, *Phil. Mag.* **4** (1959) 32.
60. L. REIMER, *Lab. Invest.* **14** (1965) 1082.
61. A. BROCKES, *Z. fur Physik* **149** (1957) 353.
62. L. REIMER and R. CHRISTENHUSZ, *Lab. Invest.* **14** (1965) 1158.
63. T. P. SCIACCA and A. G. EUBANKS, *Rev. Sci. Instrum.* **37** (1966) 1019.
64. T. NAGASAWA and K. KOBAYASHI, *J. Appl. Phys.* **41** (1970) 4279.
65. E. R. EPP, H. WEISS and A. SANTOMASSO, *Radiat. Res.* **34** (1968) 320.
66. J. W. HEAVENS, A. KELLER, J. M. POPE and D. M. ROWELL, *J. Mater. Sci.* **5** (1970) 53.
67. A. COLEBROOK and A. WINDLE, Proceedings of the Scanning Electron Microscope Systems and Applications Conference series no. 18 (Institute of Physics, London and Bristol, 1973) p. 132.
68. D. T. GRUBB and A. KELLER, *J. Mater. Sci.* **7** (1972) 822.
69. L. REIMER, *Z. Naturforsch.* **145** (1959) 566.
70. W. LIPPERT, Proceedings of the European Regional Conference on Electron Microscopy, Delft (De Nederlanske Vereniging Voor Elecktronenmicroscopie, Delft 1960) Vol 2 p. 682.
71. W. LIPPERT, *Optik* **19** (1962) 145.
72. A. COSSLETT, *J. Roy. Micros. Soc.* **79** (1960) 263.
73. B. C. HILL and G. B. HAYDON, Proceedings of the 30th Annual EMSA meeting, C. J. Arceneaux (Claitors, Los Angeles, 1972) p. 688.
74. J. W. EDIE and U. L. KARLSSON, *J. Microscopie* **13** (1972) 13.
75. G. L. CLAVER and W. H. FARNHAM, *Powder Technology* **6** (1972) 313.
76. R. E. THACH and S. S. THACH, *Biophysics J.* **11** (1971) 204.
77. G. F. BAHR, F. B. JOHNSON and E. ZEITLER, *Lab. Invest.* **14** (1965) 1115.
78. K. STENN and G. F. BAHR, *J. Histochem. Cytochem.* **18** (1970) 574.
79. G. S. Y. YEH, *J. Macromol. Sci. Phys.* **B6** (3) (1972) 451.
80. K. KOBAYASHI and K. SAKAOKU, *Lab. Invest.* **14** (1965) 1097.
81. R. HOSEMANN and S. W. BAGGCHI, "Direct Analysis of Diffraction by Matter" (North Holland, Amsterdam, 1962).
82. G. SIEGEL, Proceedings of the 7th International Congress on Electron Microscopy, Grenoble (1970) p. 221.
83. *Idem, Z. Naturforsch.* **27a** (1972) 325.
84. D. T. GRUBB and G. W. GROVES, *Phil. Mag.* **24** (1971) 815.
85. E. L. THOMAS and D. G. AST, *Polymer* **15** (1974) 37.
86. I. G. STOYANOVA, Proceedings of the 6th Congress on Electron Microscopy Kyoto 1966, (Maruzen, Tokyo) Vol **1** p. 581.
87. R. M. GLAESER, V. E. COSSLETT and U. VALDRE, *J. Microscopie* **12** (1971) 133.

88. J. A. VENABLES and D. C. BASSETT, *Nature* **214** (1967) 1107.
89. G. HONJO and M. WATANABE, *Nature* **181** (1958) 326.
90. M. G. DOBB, Proceedings of the 5th European Congress on Electron Microscopy, Manchester (Institute of Physics, London and Bristol, 1972) p 564.
91. L. W. HOBBS, Proceedings of the 25th Anniversary Meeting of the Electron Microscopy and Analysis Group, Cambridge (Institute of Physics, London and Bristol, 1971) p. 178.
92. K. KOBAYASHI and M. OHARA, Proceedings of the 6th International Congress on Electron Microscopy, Kyoto 1966 (Maruzen, Tokyo) Vol **1** p. 579.
93. L. E. THOMAS, C. J. HUMPHREYS, W. R. DUFF and D. T. GRUBB, *Radiat. Effects* **3** (1970) 89.
94. E. M. BELAVTSEVA, *Dokl. Akad. Nauk. SSSR* **125** (1959) 1005.
95. D. T. GRUBB, D.Phil. Thesis, Oxford University 1970.
96. N. A. WEIR, *Radiat. Effects* **11** (1971) 23.
97. V. F. HOLLAND and P. H. LINDENMEYER, *Science* **147** (1965) 1296.
98. G. S. Y. YEH, *J. Macromol. Sci. Phys.* **B6** (3) (1972) 451.
99. W. WILKE, W. VOGEL and R. HOSEMANN, *Kolloid Z.u.Z. Polymere* **237** (1970) 317.
100. E. L. THOMAS, S. L. SASS and E. J. KRAMER, *J. Polymer Sci. Polymer Phys.* **12** (1974) 1015.
101. J. J. POINT, *Bull. Acad. R. Belg. Cl. Sci.* **41** (1955) 982.
102. H. D. KEITH and F. J. PADDEN, *J. Polymer Sci.* **39** (1959) 101, 123.
103. A. KELLER, *ibid* **39** (1959) 151.
104. *Idem, Nature* **171** (1953) 170.
105. F. P. PRICE, *J. Polymer Sci.* **37** (1959) 71.
106. A. KELLER and D. C. BASSETT, *J. Roy. Micros. Soc.* **79** (1960) 243.
107. R. G. CLAVER, R. BUCHDAHL and R. L. MILLER, *J. Polymer Sci.* **20** (1956) 202.
108. P. H. GEIL, "Polymer Single Crystals", Polymer Reviews 5 (Interscience, New York, 1963) p. 229.
109. E. H. ANDREWS, M. W. BENNETT and A. MARKHAM, *J. Polymer Sci. A-2*, **5** (1967) 1235.
110. J. DLUGOSZ and A. KELLER, *J. Appl. Phys.* **39** (1968) 5776.
111. D. T. GRUBB, A. KELLER and G. W. GROVES, *J. Mater. Sci.* **7** (1972) 131.
112. R. W. DITCHFIELD, D. T. GRUBB and M. J. WHELAN, *Phil. Mag.* **27** (1973) 1267.
113. E. H. ANDREWS, *Proc. Roy. Soc.* **A270** (1962) 232
114. R. G. SCOTT, *J. Appl. Phys.* **28** (1957) 1089.
115. A. KELLER and E. ENGLMAN, *J. Polymer Sci.* **36** (1969) 361.
116. C. G. CANNON and P. H. HARRIS, *J. Macromol. Sci. Phys.* **B3** (1969) 357.
117. F. KHOURY, *J. Res. Nat. Bur. Stand.* **70A** (1966) 29.
118. S. F. PULLEN, E. C. FLEET, D. E. MEYER and K. THOMAS, Proceedings of the 5th European Congress on Electron Microscopy, Manchester (Institute of Physics, London and Bristol, 1972) p. 258.
119. J. DLUGOSZ, D. T. GRUBB, A. KELLER and M. B. RHODES, *J. Mater. Sci.* **7** (1972) 142.
120. J. E. BREEDON, J. F. JACKSON, M. J. MARCINKOWSKI and M. E. TAYLOR JUN, *ibid* **8** (1973) 1071.
121. A. KELLER, *Phil. Mag* **6** (1961) 63.
122. S. YAMAGUCHI, *Z. Angew. Phys.* **8** (1956) 221.
123. B. VON BORRIES and W. GLASER, *Kolloid Z.* **106** (1944) 123.
124. M. J. WHELAN, P. B. HIRSCH, R. W. HORNE and W. BOLLMANN, *Proc. Roy. Soc.* **A240** (1957) 524
125. K. KANAYA, *J. Electronmicroscopy* **3** (1955) 1.
126. B. GALE and K. F. HALE, *Brit. J. Appl. Phys.* **12** (1961) 115.
127. M. WATANABE, T. SOMEYA and Y. NAGAHAMA, Proceedings of the 5th International Congress on Electron Microscopy, Philadelphia (Academic Press, New York and London, 1962) 1, A8.
128. L. REIMER, "Elektronenmikroskopische Untersuchungs- und Präparationsmethoden" 2nd Edn (Springer-Verlag, Berlin, 1967).
129. L. REIMER, R. CHRISTENHUSZ and J. FISCHER, *Naturwissenschaften* **47** (1960) 464.
130. L. REIMER and R. CHRISTENHUSZ, *Z. Angew. Phys.* **14** (1962) 601.
131. V. K. ZWORKIN, "Electron Optics and the Electron Microscope" (Wiley, New York, 1945).
132. P. FAVARD and N. CARASSO, *J. Microscopy* **97** (1973) 59.
133. E. F. BURTON, R. S. SENNET and E. G. ELLIS, *Nature* **160** (1947) 565.
134. K. LITTLE, Proceedings of the 3rd International Conference on Electron Microscopy, London, 1954 (Royal Microscopical Soc., London, 1956) p. 165.
135. K. LITTLE, Proceedings of the 25th Anniversary Meeting of the Electron Microscopy and Analysis Group, Cambridge (Institute of Physics, London and Bristol, 1971) p. 336.
136. A. W. LEVINE, M. KAPLAN and J. FECH, *J. Polymer Sci. Chemistry* **11** (1973) 311.
137. R. M. GLAESER, *J. Ultrastructural Res.* **36** (1971) 466.
138. H. MAHL and W. WEITSCH, *Naturwissenschaften* **46** (1959) 487.
139. T. KOMODA and S. HOSOKI, Proceedings of the 6th International Congress on Electron Microscopy, Kyoto, 1966 (Maruzen, Tokyo) Vol **1** 35.
140. I. G. STOYANOVA and T. P. MOROZOVA, *Sov. Phys. Dokl.* **8** (1963) 161.
141. I. G. STOYANOVA and T. P. MARTYNENKO, *Works Laboratory* **30** (1964) 1470.
142. S. M. SALIH and V. E. COSSLETT, to be published in *Phil Mag.*
143. H. MARTIN and J. HIRSCH, *Solid State Commun.* **7** (1969) 279.

144. G. V. SPIVAK, E. I. RAU, A. E. LUKIANOV, V. I. PETROV and M. V. BICOV, Proceedings of the 5th European Regional Congress on Electron Microscopy, Manchester (Institute of Physics, London and Bristol, 1972) p. 492.
145. H. CHANZY, E. ROCH and R. VUONG, *Kolloid Z.u.Z. Polymere* **248** (1971) 1034.
146. *Idem, J. Polymer Sci. Physics* **11** (1973) 1859.
147. A. E. ENNOS, *Brit. J. Appl. Phys.* **4** (1953) 101.
148. *Idem, ibid* **5** (1954) 27.
149. H. G. HEIDE, *Lab. Invest.* **14** (1965) 1134.
150. J. ESCAIG and C. SELLA, Proceedings of the 6th International Congress on Electron Microscopy, Kyoto 1966 (Maruzen, Tokyo), Vol **1**, 177.
151. H. G. HEIDE, *Z. Angew. Physik.* **15** (1963) 116.
152. B. M. SIEGEL, *Berichte der Bunsen-Gesellschaft* **74** (1970) 1175.
153. *Idem, Phil. Trans. Roy. Soc.* **B261** (1971) 5.
154. K. ANDERSON, *J. Physics, E: Sci. Instrum.* **1** (1968) 601.
155. A. ROSE, *J. Opt. Soc. Amer.* **38** (1947) 196.
156. R. GEVERS, *Phil. Mag.* **7** (1962) 1681.
157. M. VON ARDENNE, "Tabellen zur angewandten Physik" 2nd Edn (Springer Verlag, Berlin, 1962) Vol. **1.**
158. J. SEVELY, *Compt. Rend. Acad. Sci.* **B269** (1969) 249.
159. V. MATRICARDI, G. WRAY and D. F. PARSONS, *Micron* **3** (1972) 526.
160. M. J. RICHARDSON and K. THOMAS, Proceedings of the 5th European Regional Congress on Electron Microscopy, Manchester (Institute of Physics, London and Bristol, 1972) p. 562.
161. J. A. RUSNOCK and D. HANSEN, *J. Polymer Sci.* **A3** (1965) 647.
162. C. W. HOCK, *ibid A-2* **5** (1967) 471.
163. J. H. MANLEY, *J. Ultrastructural Res.* **29** (1969)383.
164. F. FILISKO, P. NOVAK and P. H. GEIL, *J. Ultrastructural Res.* **38** (1972) 102.
165. G. DUPUOY, F. PERRIER and P. VERDIER, *Compt. Rend. Acad. Sci.* **262B** (1966) 1063.
166. H. M. JOHNSON and D. F. PARSONS, *J. Microscopy* **90** (1969) 199.
167. P. N. T. UNWIN, *Proc. Roy. Soc.* **A239** (1972) 327.
168. P. W. HAWKES, Ed. "Image Processing and Computer Aided Design in Electron Optics" (Academic Press, London and New York, 1973).
169. R. C. VALENTINE and N. G. WRIGLEY, *Nature* **203** (1964) 713.
170. R. C. VALENTINE, in "Advances in Optics and Electron Microscopy", edited by R. Barer and V. E. Cosslett, **1** (Academic Press, New York and London, 1966) p. 180.
171. G. C. FARNELL and R. B. FLINT, *J. Microscopy* **97** (1973) 271.
172. H. F. PREMSELA and W. KUHL, Phil. Scient. and Anal. Equipment, Bulletin E.M. 30, 1968.
173. G. T. REYNOLDS, in "Advances in Optics and Electron Microscopy", edited by R. Barer and V. E. Cosslett, **2** (Academic Press, New York and London, 1968) p. 1.
174. C. A. ENGLISH and J. A. VENABLES, Proceedings of the 5th European Congress on Electron Microscopy, Manchester (Institute of Physics, London and Bristol, 1972) p. 172.
175. E. L. THOMAS and S. DANYLUK, *J. Phys. E: Sci. Instrum.* **4** (1971) 843.
176. H. F. PREMSELA and A. JORE, Proceedings of the 25th Anniversary Meeting of the Electron Microscopy and Analysis Group, Cambridge (Institute of Physics, London and Bristol, 1971), p. 38.
177. E. RUSKA, in "Advances in Optics and Electron Microscopy", edited by R. Barer and V. E. Cosslett, **1** (Academic Press, New York and London, 1966) p. 115.
178. H. P. ZINGSHEIM and L. BACHMANN, *Kolloid Z.u.Z. Polymere* **246** (1971) 561.
179. D. M. SADLER and A. KELLER, *ibid* **239** (1970) 641.
180. D. C. BASSETT and A. KELLER, *Phil. Mag.* **6** (1961) 345.

Received 19 March and accepted 21 March 1974.